Catalysis Letters 35 (1995) 361–372

Catalytic decomposition of nitrous oxide on strontium-substituted La_2CuO_4 materials

S. Subramanian and C.S. Swamy

Catalysis Division, Department of Chemistry, Indian Institute of Technology,
Madras 600 036, India

Received 16 March 1995; accepted 8 August 1995

Catalytic decomposition of nitrous oxide (N_2O) to N_2 and O_2 has been studied on a series of solid oxide solutions of La, Sr and Cu according to the nominal formula $La_{2-x}Sr_xCuO_4$ ($0 \leqslant x \leqslant 1$). The reaction has been carried out in a fixed bed, glass static reactor with gas-recirculation facility. The kinetics of decomposition has been studied in the temperature range 250–480°C. Among the catalysts studied, $x = 0.15$ and $x = 1.0$ showed higher catalytic activity (in terms of %conversion). The enhanced activity of the above systems has been explained on the basis of mixed valency of copper (Cu^{2+}/Cu^{3+}) and anion vacancies respectively.

Keywords: nitrous oxide decomposition; lanthanum–strontium–copper oxide; copper mixed valency; anion vacancies

1. Introduction

Copper containing ternary oxides crystallising in the K_2NiF_4 structure have been found to exhibit interesting structural, solid state and catalytic properties [1,2]. The material La_2CuO_4 and its Sr/Ba-doped analogues have recently been the subject of active research due to their unusual electronic properties, particularly the observation of superconductivity at about 40 K [3]. The high electronic conductivity of these compounds is due to the ability of copper to take different coordinations as well as the formation of mixed valency states, which may have an effect on the catalytic activity. The activity of the Sr-doped La_2CuO_4 materials has been tested towards the oxidation of CO [4], decomposition of NO [5] and decomposition of isopropyl alcohol [6]. They have been found to show high catalytic activity for CO-oxidation which is comparable to that of highly dispersed Pt/alumina fume abatement catalyst. $La_{1.85}Sr_{0.15}CuO_4$ has been found to be more active than La_2CuO_4 and $CuAlO_2$ for the catalytic decomposition of nitrous oxide [7]. The improvement observed in the catalytic activity of La_2CuO_4 with the doping of small amounts of strontium in the lattice instigated a detailed investigation of relative catalytic efficiencies of the members of the solid solution system, $La_{2-x}Sr_xCuO_{4-\delta}$

($0 \leqslant x \leqslant 1$) towards the decomposition of N_2O into N_2 and O_2. The materials have been characterised by various techniques – XRD, iodometry, electrical resistivity – and studied for the decomposition of N_2O at 50 Torr initial pressure. The activity change has been explained by the presence of a mixed valent system and anion vacancies.

2. Synthesis and characterisation

2.1. SYNTHESIS

The catalysts prepared were of the formula $La_{2-x}Sr_xCuO_{4-\delta}$ ($x = 0.1, 0.1, 0.15, 0.2, 0.4, 0.6, 0.8$ and 1.0). Generally, they were synthesised by the solid state reaction route. Stoichiometric quantities of preheated La_2O_3 (heated at 1000°C/24 h and cooled in a vacuum desiccator), $SrCO_3$ and CuO were mixed well using acetone and heated at 900°C for 12 h and later calcined at temperatures ranging from 1000–1200°C.

2.2. PHYSICAL PROPERTIES

X-ray diffraction analysis (Cu K_α) of the resultant materials was carried out to confirm the formation of the required single phase. The lattice parameters were calculated by the least squares refinement method using a FORTRAN program. The least squares fit was carried out on the basis of tetragonal symmetry for all the compositions except for La_2CuO_4 and $La_{1.9}Sr_{0.1}CuO_4$ which were fitted on the basis of orthorhombic symmetry. The lattice parameters of the members of the series are given in table 1. The tolerance factor (t') for these compounds given in table 1 has

Table 1
Structural and solid state properties of $La_{2-x}Sr_xCuO_{4-\delta}$ materials

Material	Lattice parameters (Å)			Tolerance factor [a] (t')	AON [b] of copper	Oxygen deficiency (δ)	Resistivity ρ_{300K} (mΩ cm)
	a	b	c				
La_2CuO_4	5.366	5.402	13.150	0.860	2.00	0.0	67.0
$La_{1.9}Sr_{0.1}CuO_4$	5.351	5.368	12.200	0.862	2.10	0.0	17.0
$La_{1.85}Sr_{0.15}CuO_4$	3.774	–	13.231	0.863	2.15	0.0	2.5
$La_{1.8}Sr_{0.2}CuO_{3.96}$	3.775	–	13.245	0.864	2.12	0.04	3.9
$La_{1.6}Sr_{0.4}CuO_{3.85}$	3.776	–	13.225	0.867	2.10	0.15	7.6
$La_{1.5}Sr_{0.5}CuO_{3.79}$	3.773	–	13.204	0.869	2.08	0.21	8.3
$La_{1.4}Sr_{0.6}CuO_{3.74}$	3.774	–	13.175	0.871	2.07	0.26	11.0
$La_{1.2}Sr_{0.8}CuO_{3.62}$	3.773	–	13.110	0.874	2.04	0.38	17.0
$La_{1.0}Sr_{1.0}CuO_{3.50}$	3.767	–	13.002	0.878	2.00	0.50	40.0

[a] $t' = r_A + r_O/\sqrt{2}(r_B + r_O)$.
[b] AON: average oxidation number.

been calculated by taking r_a as the weight average ionic radii of La and Sr. The tolerance factor values of these Sr-substituted compounds in this series are found be in the range of 0.860–0.878, which fall within the range of allowed tolerance factor limits for K_2NiF_4 type lattice. The electrical properties of the prepared solid solutions were examined at room temperature using a four-probe setup. The room temperature resistivity has been found to be minimum for the composition $x = 0.15$ (table 1). The BET (N_2) method was used to evaluate the surface area of the solid solutions. They were found to possess low surface areas, in the range of 1.0–2.0 $m^2\ g^{-1}$ because of the high temperature employed in the synthesis.

2.3. CHEMICAL COMPOSITION ANALYSIS

The bulk compositions of the materials were determined by wet-chemical analysis. The lanthanum content of the compounds was estimated gravimetrically by dissolution of the compounds in dilute HCl, precipitating the metal as oxlate and igniting the exalates to the corresponding oxides. The Sr-contents of the samples were estimated by the inductively coupled plasma emission spectroscopy (ICPES) method. About 10–20 mg of accurately weighed sample was dissolved in minimum quantity of HCl and made upto 100 ml. The Sr-content of the solution was calculated from the intensity of the emission spectrum. The divalent and trivalent copper contents of the $La_{2-x}Sr_xCuO_{4-\delta}$ series were estimated by iodometry as per the procedure adopted by Harris et al. [8]. The Cu^{3+} may also correspond to Cu^{2+} and a positive hole of oxygen [9]. In that case iodometry values correspond to the total oxidative power $(Cu-O)^+$ of the system. Oxygen non-stoichiometry values given in table 1 were calculated from the amount of Cu^{2+} and Cu^{3+} assuming that other ions are in the most stable oxidation states, viz. La^{3+}, Sr^{2+} and O^{2-}.

2.4. KINETIC AND CATALYTIC STUDIES

The decomposition of nitrous oxide has been done in an all-glass static gas-recirculatory reactor manifold. The catalysts (1 g) are subjected to the following pretreatment in between the kinetic runs: (1) evacuation at 500°C at 10^{-6} Torr for 2 h, (2) treatment with 100 Torr oxygen at the reaction temperature, and (3) mild evacuation at 10^{-3} Torr to remove gas phase and weakly adsorbed oxygen. The decomposition has been studied at 50 Torr initial pressure of N_2O. Gas samples from the catalytic reactor were taken using a micro syringe and analysed by quadrupole mass spectrometer. The products identified were only N_2 and O_2. The conversion has been limited to $<25\%$ to obtain diffusion-free kinetic behaviour. Kinetic measurements were repeated till reproducible activity was obtained. In certain cases, due to the initial adsorption of oxygen from N_2O decomposition by the catalyst surface, the pressure reading may not absolutely correspond to the kinetic changes. In such cases, corrections for the oxygen adsorption had to be incorporated as reported by Louis Raj et al. [10].

3. Results and discussion

The solid solution system is fairly active toward the decomposition reaction in the temperature range 300–450°C. Nitrous oxide decomposes as

$$N_2O \rightarrow N_2 + O_2 \tag{1}$$

The mechanism of this reaction involves the following steps as proposed by Winter [11]:

$$N_2O_{(g)} \rightarrow N_2O_{(ads)} \tag{2}$$

$$N_2O_{(ads)} + e^- \rightarrow N_2O^-_{(ads)} \tag{3}$$

$$N_2O^-_{(ads)} \rightarrow N_{2(g)} + O^-_{(ads)} \tag{4}$$

$$O^-_{(ads)} + O^-_{(ads)} \rightarrow O_{2(g)} + 2e^- \tag{5}$$

$$\dot{O}^- + N_2O \rightarrow O_{2(g)} + N_{2(g)} + 2e^- \tag{6}$$

Adsorption of N_2O (step (2)) and desorption of the product oxygen (O^-_{ads}) as molecular oxygen (step (5)) are the important steps in governing the rate of the reaction. The kinetic parameters of N_2O decomposition have been derived using the following rate equations:

$$\ln\left(\frac{a}{a-x}\right) = k_1 t, \tag{7}$$

$$\left(\tfrac{1}{2}a\right)\ln\left(\frac{a^{1/2}+x^{1/2}}{a^{1/2}+x^{1/2}}\right) - (2x)^{1/2} = k_2 t, \tag{8}$$

$$\ln\left(\frac{a}{a-x}\right) - b\left[\left(\tfrac{1}{2}a\right)\ln\left(\frac{a^{1/2}+x^{1/2}}{a^{1/2}+x^{1/2}}\right) - (2x)^{1/2}\right] = k_3 t, \tag{9}$$

where $a = P^0_{N_2O}$, initial pressure of N_2O, $x = P^t_{N_2O}$, pressure of N_2O at time t, $x/2 = P^t_{O_2}$, pressure of oxygen produced at time t. Rate equation (7) corresponds to no inhibition by product oxygen or simple dependence of the rate on the concentration of N_2O molecules (step (2)). Rate equation (8) corresponds to strong inhibition by oxygen or the dependence of rate on the desorption of adsorbed oxygen (step (5)). Rate equation (9) represents weak inhibition on the decomposition kinetics by oxygen. Plots of LHS versus time will indicate the rate law applicable for the decomposition. The experimental data of the decomposition of N_2O to N_2 and O_2 at 50 Torr initial pressure of N_2O has been best fitted according to no inhibition by product oxygen on the decomposition kinetics. The fitting of the experimental data was done by the least squares regression method using a FORTRAN program. Separate experiments with initial mixtures of N_2O and O_2 indicated that the rate is not hindered by the presence of oxygen.

Typical kinetic plots for the decomposition on $La_{1.85}Sr_{0.15}CuO_4$ and $La_{1.0}Sr_{1.0}CuO_{3.5}$ are shown in fig. 1. The value of rate constants and the Arrhenius parameters are given in table 2. The activation energy and frequency factor values have been calculated from the Arrhenius plot (fig. 2).

Fig. 3 depicts the variation of % conversion at various temperatures for different strontium substitution levels. The catalytic activity as measured by the %conversion at a constant temperature (400°C) at 30 min reaction time for 1 g of the catalysts, against the strontium content is shown in fig. 4. From these figures it is clear that the addition of Sr decreases the temperature at which appreciable conversion is observed. In the case of La_2CuO_4, minimum conversion has been noted only above 400°C whereas $LaSrCuO_{3.5}$ is active at about 280°C. Maximum catalytic activity, among the members of the solid solution, is exhibited by the low Sr-doped compound $La_{1.85}Sr_{0.15}CuO_4$ and the maximum Sr-doped compound, $LaSrCuO_{3.5}$.

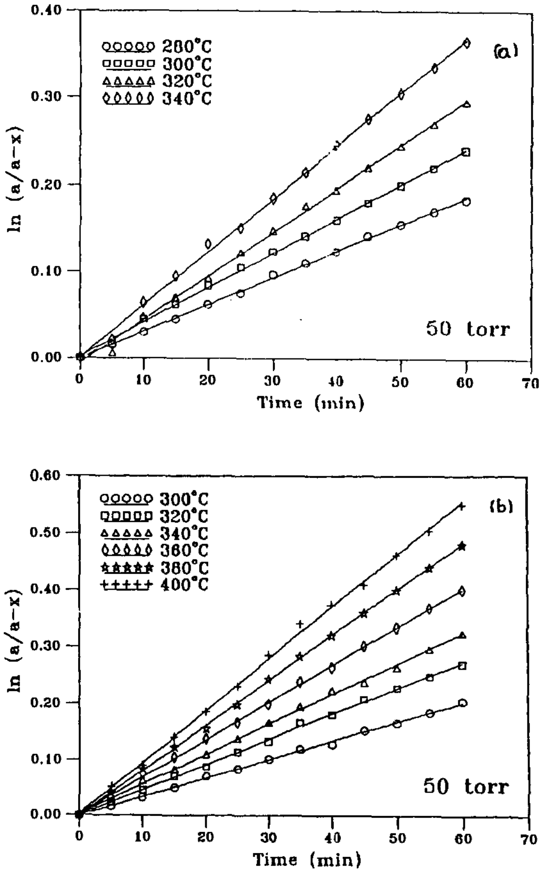

Fig. 1. Kinetic plots for the decomposition of N_2O on (a) $La_{1.85}Sr_{0.15}CuO_4$ and (b) $La_{1.0}Sr_{1.0}CuO_{3.5}$.

Table 2
Kinetic and Arrhenius parameters for the decomposition of N_2O on $La_{2-x}Sr_xCuO_{4-\delta}$ catalysts ($P_{N_2O} = 50$ Torr)

Catalyst	Reaction temp. (°C)	Rate constant $k \times 10^3$ (min^{-1})	E_a (kJmol^{-1})	ln A	% conversion at 30 min reaction time
La_2CuO_4	420	1.57	74.8	6.4	4.8
	440	2.22			6.4
	460	2.78			8.4
$La_{1.9}Sr_{0.1}CuO_4$	340	3.35	47.2	3.6	10.0
	360	4.70			14.0
	380	6.00			18.0
	400	8.13			21.6
$La_{1.85}Sr_{0.15}CuO_4$	280	3.11	31.6	1.1	9.2
	300	3.98			11.6
	320	5.04			15.2
	340	6.07			19.2
$La_{1.8}Sr_{0.2}CuO_{3.96}$	400	2.45	59.5	4.7	7.2
	420	3.52			9.2
	440	4.61			12.0
	480	5.89			15.6
$La_{1.6}Sr_{0.4}CuO_{3.85}$	380	2.61	54.7	4.1	7.8
	400	3.66			10.8
	420	4.51			12.8
	440	6.20			17.2
	460	7.11			19.6
$La_{1.5}Sr_{0.5}CuO_{3.79}$	380	2.83	50.7	3.5	8.8
	400	3.96			11.2
	420	4.90			14.4
	440	6.80			18.4
	460	7.89			21.6
$La_{1.4}Sr_{0.6}CuO_{3.74}$	340	3.93	42.7	2.9	10.0
	360	5.13			14.0
	380	6.81			17.6
	400	8.23			22.0
$La_{1.2}Sr_{0.8}CuO_{3.62}$	320	3.52	34.0	1.2	8.4
	340	4.46			12.8
	360	5.39			16.4
	380	6.59			18.8
	400	8.01			21.6
$La_{1.0}Sr_{1.0}CuO_{3.50}$	300	3.36	30.3	0.7	9.6
	320	4.53			12.4
	340	5.34			15.2
	360	6.63			18.2
	380	7.98			21.6

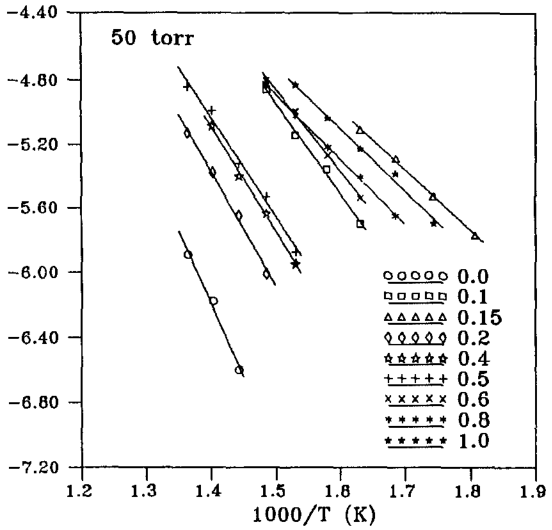

Fig. 2. Arrhenius plot for the decomposition of N_2O on $La_{2-x}Sr_xCuO_{4-\delta}$ catalysts.

The parent compound of the present series, La_2CuO_4 is stoichiometric with respect to oxygen. The positive charge deficiency at the La^{3+} site due to the substitution of Sr^{2+} can be compensated by the oxidation of Cu^{2+} to Cu^{3+} or by a defect structure with oxygen vacancies [1]. Temperature programmed reduction using H_2/He indicates that upto strontium substitution level of $x = 0.15$, the compounds are stoichiometric and the charge imbalance is mainly compensated by the oxidation of Cu^{2+} to Cu^{3+}. The amount of Cu^{3+} content, estimated by iodometry has

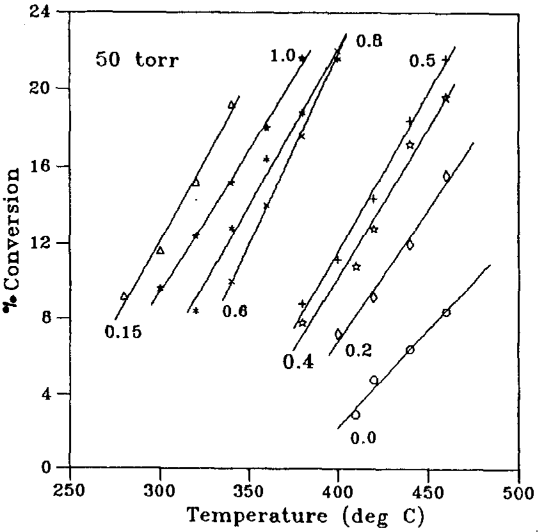

Fig. 3. Variation of %conversion of N_2O with temperature on $La_{2-x}Sr_xCuO_{4-\delta}$ catalysts.

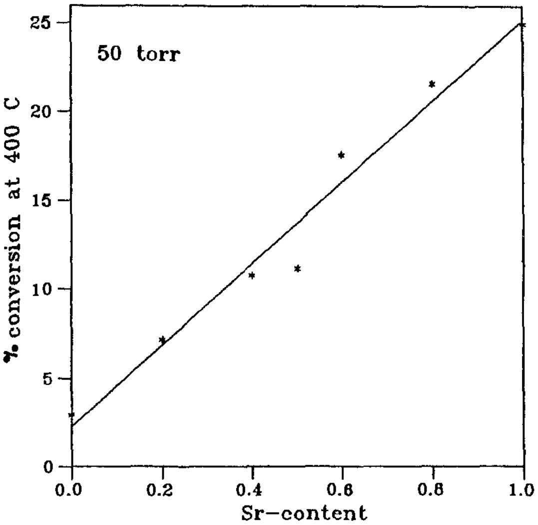

Fig. 4. Variation of %conversion of N_2O at 30 min reaction time at 400°C for $La_{2-x}Sr_xCuO_{4-\delta}$ catalysts.

been found equal to the strontium substitution amount (table 1). For compositions, $x>0.15$, complete oxidation of Cu^{2+} to Cu^{3+} does not occur under the synthesis conditions. Therefore, a defect structure with large oxygen vacancies seems to stabilise the K_2NiF_4 structure.

The members of the $La_{2-x}Sr_xCuO_{4-\delta}$ series were analysed by X-ray photoelectron spectroscopy to get an idea about the oxidation state of the individual elements and also to determine the surface composition of the catalysts; the results are published elsewhere [12]. The shifting of the Cu $2p_{3/2}$ peak to higher binding energy region (934.5 eV) compared to 933.5 eV for CuO and the reduction in the ratio between the intensities of the main and satellite peaks indicate the presence of Cu^{3+}. However, no significant chemical shifts, among the members of the La-Sr-Cu-O series, have been observed and also the expected positive shift in Cu $2p_{3/2}$ binding energy would hardly exceed the experimental error in the energy resolution of the spectrometer employed (<0.7 eV). Absence of the peak at the higher binding energy region corresponding to Cu^{3+} by XPS or by other spectroscopic methods could not be taken as a proof for the non-existence of Cu^{3+}, as it has also been reported that the surface of these materials undergoes extensive damage by keeping under ultrahigh vacuum and irradiation by photons, electrons and other high energy sources, which results in the loss of oxygen from the surface layers and the consequent reduction of Cu^{3+} [13].

The sharp increase in the conversion levels of N_2O, on going from strontium substitution level of $x = 0.0$ to $x = 0.15$, could only be corroborated to the formation of Cu^{2+}/Cu^{3+} redox systems as no oxygen vacancy creation occurs by the substitution of La^{3+} by Sr^{2+}. The mechanism of N_2O decomposition given above involves the activation of N_2O molecule by the donation of an electron from the catalyst surface (step (3)). Steps (5) and (6) indicate the desorption path of oxygen, by donation of a pair of electrons to the surface. Adsorption of N_2O and desorption of O_2 are more favoured on p-type oxides due to its accumulative nature [14] and on catalysts containing active metal ions in mixed valency states [15,16]. The reactivity of Cu^{3+} can be more than that of Cu^{2+} since it has d^8 electronic configuration which is less stable than the d^9 electronic configuration in the Cu^{2+} system. The decomposition of N_2O according to the above mechanism, demands easy transfer of electrons from the catalyst. In $La_{2-x}Sr_xCuO_{4-\delta}$ compounds, the electron transfer between the copper ions bound by an oxygen can take place through superexchange as follows:

$$Cu^{2+}\text{–O–}Cu^{3+} \leftrightarrow Cu^{3+}\text{–O–}Cu^{2+} \tag{10}$$

This exchange, known as Zener double exchange (ZDE), accounts for an average oxidation state of copper ions at least in the time scale of reaction of N_2O and reaches a maximum for an angle Cu–O–Cu of π radian, i.e., for the cubic structure. Such an average oxidation state of copper can facilitate the adsorption–desorption of the reactants whereas individual Cu^{2+} ions in their discrete spin and oxidation states lead to an adsorption process that is too strong or too weak for a catalytic reaction to take place. Thus the redox couple, Cu^{2+}/Cu^{3+}, by its capacity to facilitate easy charge-transfer in the N_2O decomposition reaction enhances the activity. The high electrical conductivity of $La_{1.85}Sr_{0.15}CuO_4$ makes transfer of several electrons to and through one active centre possible without grossly upsetting the local equilibrium valence situation. Low electrical conductivity is most likely to limit the charge transfer processes at the surface of the compositions close to stoichiometric La_2CuO_4. Similar kind of active sites, viz. Mn^{3+}/Mn^{4+} in $La_{1-x}Sr_xMnO_3$ [16], Ni^{2+}/Ni^{3+} in $La_{2-x}Sr_xNiO_4$ [17] and Co^{2+}/Co^{3+} in $La_{2-x}Sr_xCoO_4$ [18], have been proposed to operate for various catalytic reactions. Correlation of catalytic activity with Cu^{3+} concentration has also been reported for the system $La_{2-x}Sr_xCuO_4$ in the decomposition of nitric oxide [5] and the dehydrogenation of isopropyl alcohol [6].

For compositions with $x \geqslant 0.2$, the defects have a significant effect on the imbalance of stress and charge in the structure. The enthalpy of the vacancy filling oxidation reaction increases for these compositions [19]. This is because of their effect in relieving the stress and charge imbalance in the Cu–O–Cu planes. Thus in the case of materials with $x \geqslant 0.2$, the charge imbalance arising out of substitution of divalent strontium on trivalent lanthanum sites has been compensated by the formation of oxygen vacancies as

$$x\mathrm{SrO} \xrightarrow{\mathrm{La_2O_3}} x\mathrm{Sr_{La}} + x\mathrm{O_o} + \tfrac{1}{2}x\mathrm{V_o''} \tag{11}$$

By interaction with oxygen in the ambient, the oxygen vacancies may be partially or fully filled and replaced by holes as the charge compensating effect,

$$V_o'' + \tfrac{1}{2}O_2 \rightleftharpoons O_o + 2h \tag{12}$$

Both oxygen vacancies and holes are involved in the charge compensation of the acceptors. The oxygen vacancies in Sr-doped La_2CuO_4 are preferentially located in the basal Cu–O planes [1]. Thus in the case of catalysts with Sr-content $x \geqslant 0.2$, the N_2O molecule can be adsorbed on the oxygen vacancies ($e^-/\square_s^-$) or on surface vacant sites ($\square_s^-$) [20],

$$e^-/\square_s + N_2O \rightleftharpoons N_2O^-/\square_s^- \tag{13}$$

or

$$\square_s^- + N_2O \rightleftharpoons N_2O/\square_s^- \tag{14}$$

followed by a charge-transfer in the adsorption complex,

$$(O^{2-}/\square_s^-) + (N_2O/\square_s^-) \rightleftharpoons (O^-/\square_s^-) + (N_2O^-/\square_s^-) \tag{15}$$

The charged adsorption complex then decomposes as

$$N_2O^-/\square_s^- \rightarrow N_2 + O^-/\square_s^- \tag{16}$$

The O^- ion migrates across the matrix by charge exchange,

$$(O^-/\square_s^-)_1 + (O^2/\square_s^-)_2 \rightleftharpoons (O^{2-}/\square_s^-)_1 + (O^-/\square_s^-)_2 \tag{17}$$

The subscripts 1 and 2 refer to different sites. The migration continues till the singly charged oxygen species collide in the surface by appearing on adjacent sites, desorbing as gaseous O_2 and leaving a surface R_2 center,

$$2(O^-/\square_s^-) \rightarrow O_2(g) + 2(e^-/\square_s^-) \tag{18}$$

The dependence of reaction rate ($k \times 10^3$) at 400°C and E_a on the values of δ is shown in fig. 5. The number of anion vacancies in La_2CuO_4 increases upon substitution by strontium. Thus the activity increase could be attributed to the increase in the number of vacancies with the Sr-substitution. $LaSrCuO_{3.5}$ possessing highest number of oxygen vacancies in the lattice thus exhibits maximum catalytic activity. The decrease in E_a with an increase in δ implies that the activity is related to the ease of oxygen removal in the desorbed state. Oxygen non-stoichiometry (δ) is also closely connected with the tolerance factor, t'. The activation energy decreases with increase in tolerance factor value (fig. 5). Shimizu [21] has shown that the binding energy of oxygen in a series of perovskite type oxides decreases with increase of tolerance factor and hence promotes oxygen vacancies. Thus the activity increase can be attributed to the increase in the number of anion vacancies. The observation that E_a decreases with increase in tolerance factor supports the deduction that activity is related to the easiness of oxygen desorption process.

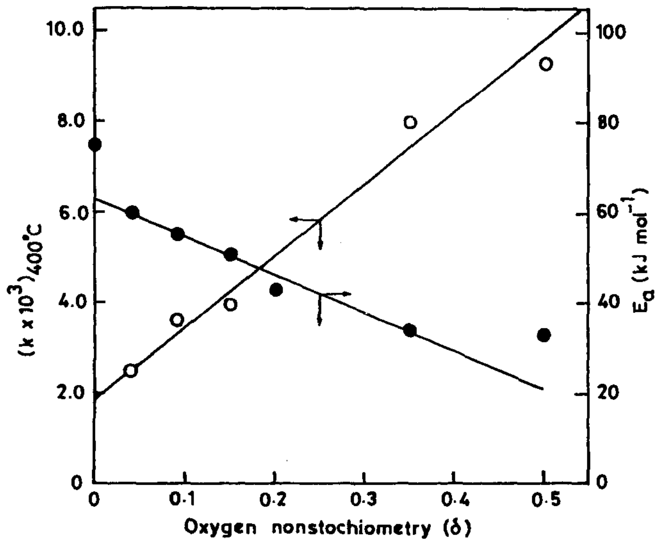

Fig. 5. Variation of E_a and $k_{400°C}$ with oxygen non-stoichiometry (δ).

4. Conclusions

The catalytic activity of the Sr-substituted La_2CuO_4 compounds has been investigated for the decomposition of N_2O. The kinetics of decomposition follows first-order no inhibition by oxygen mechanism. The catalysts are active in the temperature range 300–400°C.

In the series $La_{2-x}Sr_xCuO_{4-\delta}$, $La_{1.85}Sr_{0.15}CuO_4$ and $LaSrCuO_{3.5}$ have been found to exhibit maximum catalytic activity. The sharp increase in activity for the composition $x = 0.15$ can be explained by the presence of Cu^{2+}/Cu^{3+} redox centers which, in turn, are responsible for the maximum distortion in crystal symmetry and higher electrical conductivity. The increase in the activity along the series from $x = 0.2$ to $x = 1.0$ is due to the increase in the number of oxygen vacancies, which can be the adsorption sites for the N_2O molecules. $LaSrCuO_{3.5}$, which possesses largest number of vacancies, shows higher catalytic activity.

Acknowledgement

One of the authors (SS) thanks the Programme Management Board (PMB) of Department of Science and Technology (DST) for the National Superconductivity Fellowship (NSF). The authors also gratefully acknowledge Air Products and Chemicals Inc., USA for the financial assistance.

References

[1] N. Nguyen, J. Choisnet, M. Hervieu and B. Raveau, J. Solid State Chem. 39 (1981) 120.

[2] C.S. Swamy and J. Christopher, Catal. Rev. Sci. Eng. 34 (1992) 409.
[3] J.G. Bednorz and K.A. Muller, Z. Phys. B 64 (1986) 181.
[4] S. Rajadurai, J.J. Carberry, B. Li and C.B. Alcock, J. Catal. 131 (1991) 582.
[5] H. Yasuda, N. Misuno and M. Misuno, J. Chem. Soc. Chem. Commun. (1990) 1044.
[6] R. Jayalakshmi, B. Jagganadhaswamy, K. Rengaraj and B. Sivasankar, Bull. Chem. Soc. Jpn. 63 (1990) 2970.
[7] J. Christopher and C.S. Swamy, J. Mol. Catal. 62 (1990) 69.
[8] D.C. Harris and T.A. Hewston, J. Solid State Chem. 69 (1987) 182.
[9] T. Takahashi, F. Maeda, H. Arai, H.K. Yoshida, Y. Okabe, T. Susuki, H. Hosoya, A. Fujimori, T. Shidava, T. Koide, T. Miyahava, M. Onoda, S. Shamoto and M. Saito, Phys. Rev. B 36 (1987) 5686.
[10] S. Louis Raj, V. Srinivasan and B. Viswanathan, Curr. Sci. 49 (1980) 628.
[11] E.R.S. Winter, J. Catal. 15 (1969) 144.
[12] S. Subramanian and C.S. Swamy, unpublished.
[13] M.G. Ramsey and F.P. Netzer, Mater. Sci. Eng. B 2 (1989) 269.
[14] B. Viswanathan, Ind. Chem. Manufacturer 9 (1980) 1.
[15] J.M. Thomas and W.J. Thomas, in: *Introduction to the Principles of Heterogeneous Catalysis* (Academic Press, London, 1967) p. 269.
[16] S. Louis Rai and V. Srinivasan, J. Catal. 75 (1982) 185.
[17] T. Nitadori, M. Muramatsu and M. Misuno, Bull. Chem. Soc. Jpn. 61 (1988) 3831.
[18] T. Nitadori and M. Misuno, Chem. Lett. (1986) 1255.
[19] D.J.L. Hong and D.M. Smyth, J. Solid State Chem. 102 (1993) 250.
[20] E.R.S. Winter, J. Catal. 19 (1970) 32.
[21] T. Shimizu, Chem. Lett. (1980) 1.